$Co_{2+x}Ti_{1-x}O_4$ Nano-Octahedrons as High Performance Anode for Lithium-ion Batteries

Zheng Xing, Xiang Ji, Yulong Zhao, Haipeng Ren, Yichen Deng, Zhicheng Ju*, Quanchao Zhuang

School of Materials Science and Engineering, China University of Mining and Technology, Xuzhou, Jiangsu 221116, P. R. China.

Contents:

Corresponding author Tel.: +86 51683591877. E-mail address: juzc@cumt.edu.cn (Z. Ju).

To discuss the relationship of the morphology structure with the electrochemical performance of Co_2TiO_4 nanoparticles, a set of experiments were carried out as supplement. The Suspension liquid 1 remained unchanged, and the components of Solution 2 were varied as shown in Table S1.

Table S1. Components used to prepare Solution 2 in the contrast experiments.

Typical	0.03 g $CoCl_2 \cdot 6H_2O$	0.1 g glucose	0.05 g $H_3NO \cdot HCl$	10 ml H_2O
Sample 1	0.03 g $CoCl_2 \cdot 6H_2O$	0	0	10 ml H_2O
Sample 2	0.03 g $CoCl_2 \cdot 6H_2O$	0	0.05 g $H_3NO \cdot HCl$	10 ml H_2O
Sample 3	0.03 g $CoCl_2 \cdot 6H_2O$	0.1 g glucose	0	10 ml H_2O
Sample 4	0.03 g $CoCl_2 \cdot 6H_2O$	0.1 g glucose	0.0432 g Urea	10 ml H_2O

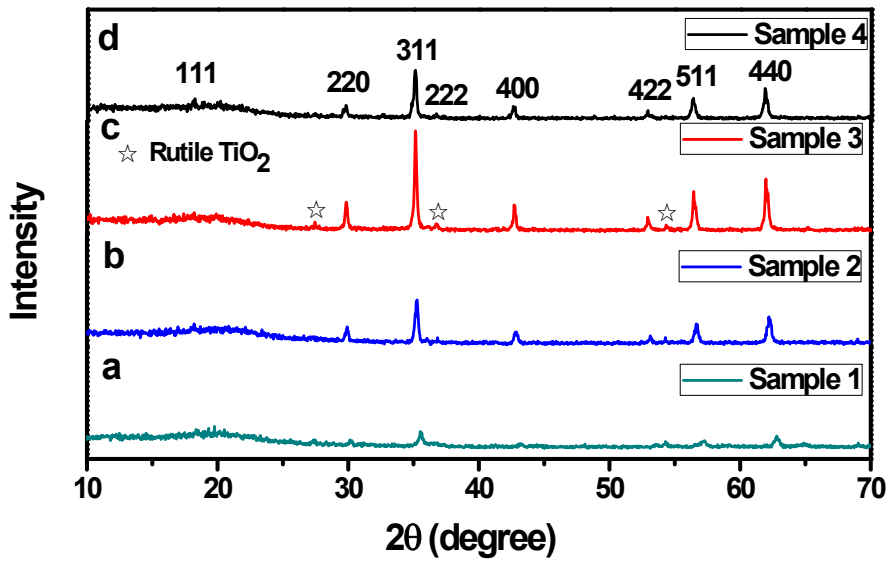

Figure S1. XRD patterns of the contrast experiments.

According to the XRD patterns of the contrast experiment, Co_2TiO_4 could be clearly observed in all the four samples. Moreover, a small amount of rutile TiO_2 could be observed in sample 3 in which no $H_3NO{\cdot}HCl$ was added.

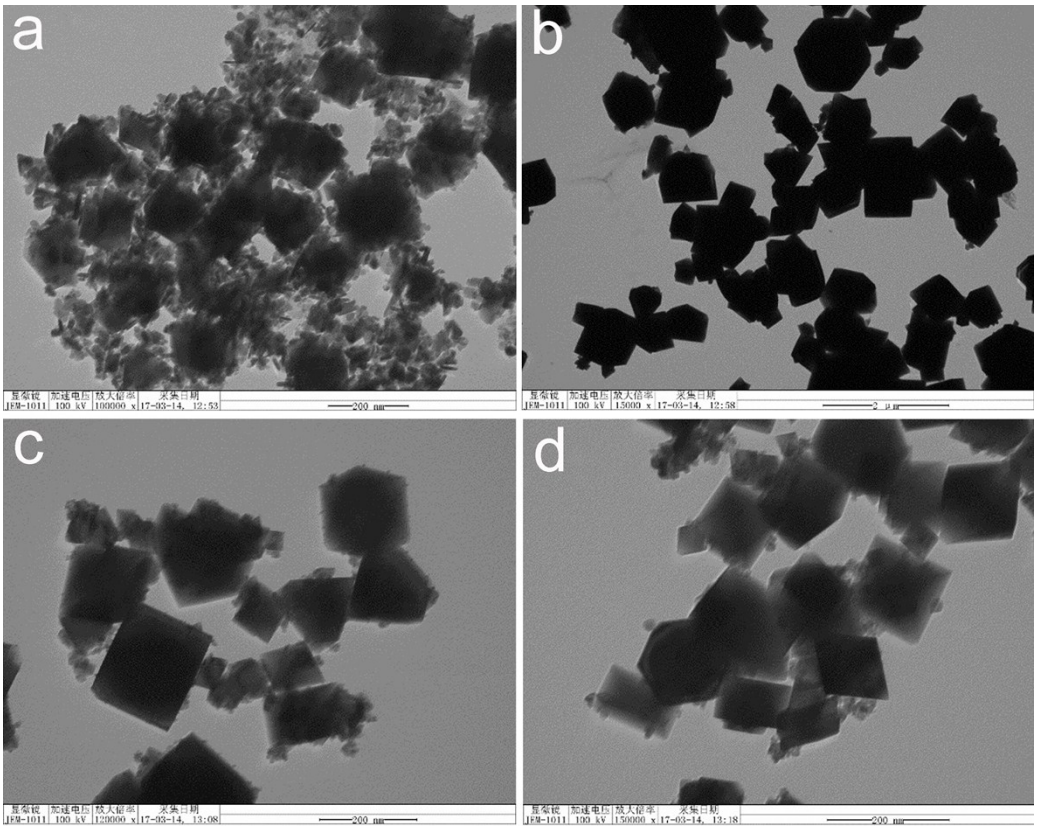

Figure S2. SEM images of the contrast experiments.

The SEM images of the contrast experiments were shown in Figure S2. Figure S2a shows the product fabricated without both glucose and $H_3NO{\cdot}HCl$; the particle size distribution of sample 1 is rather broad from tens of nano-meters to 200 nm; a part of the particles possessed octahedron morphologies. Figure S2b shows the product fabricated without glucose; the $Co_{2+x}Ti_{1-x}O_4$ product presents quite large particle size (600 nm - 1μm) which implies that the glucose played the major role in controlling the size of the octahedrons. In sample 3 (Figure S2c), octahedrons and tetrahedrons with size of about 100 – 200 nm could be observed with a part of small particles. The morphology of sample 4 (Figure S2d) is similar as the typical sample, which suggests that the coexistence of the glucose and NH_4^+ is necessary for synthesis $Co_{2+x}Ti_{1-x}O_4$ nano-octahedrons. This result implies that the ultimate shape of crystal could be controlled by using different reagents.

To research the relationship with the morphology and electrochemical performance, we applied sample 1 and 2 as active substance to test the charge/discharge properties. As shown in Figure S3a and S3b, respectively. The first discharge capacities of sample 1 and 2 are 1305 and 1386 mAh/g, respectively. The discharge capacity of sample 1 with nonuniform particle size gradually decayed to ~540 mAh/g at the 10th cycle and kept at ~480 mAh/g after 30 cycles. The discharge capacity of sample 2 with large particle size drastically dropped to ~400 mAh/g after 5 cycles and finally delivered ~270 mAh/g at the 30th cycle. In this case, $Co_{2+x}Ti_{1-x}O_4$ particles with nonuniform size and large size both possessed stable charge/discharge capacities after 10th cycle, and the specific capacities of both sample were lower than the typical sample.

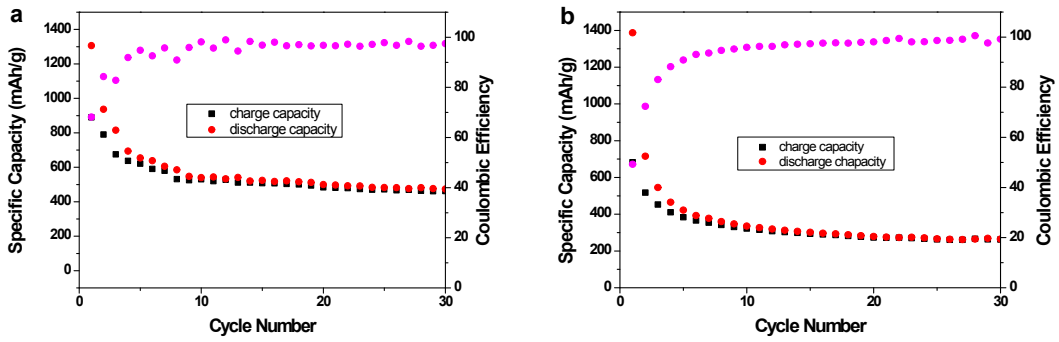

Figure S3. Specific charge/discharge capacity versus cycle number of the contrast samples in the voltage range 0.01-3.0 V at current rate of 100 mA·g^{-1}. a. Sample 1. b. Sample 2.

To determine the component content of the smaller irregular particles, we applied EDX by STEM mode on Tecnai G2 F20 Transmission Electron Microscopy in which the convergent beam region is smaller than 5nm. We select several points on small irregular particles and nano-octahedrons to analyze the component content. The figure below show the TEM and dark field image of selected area. We chose four points in which O1, O4 were irregular particles and O2, O3 were nano-octahedrons.

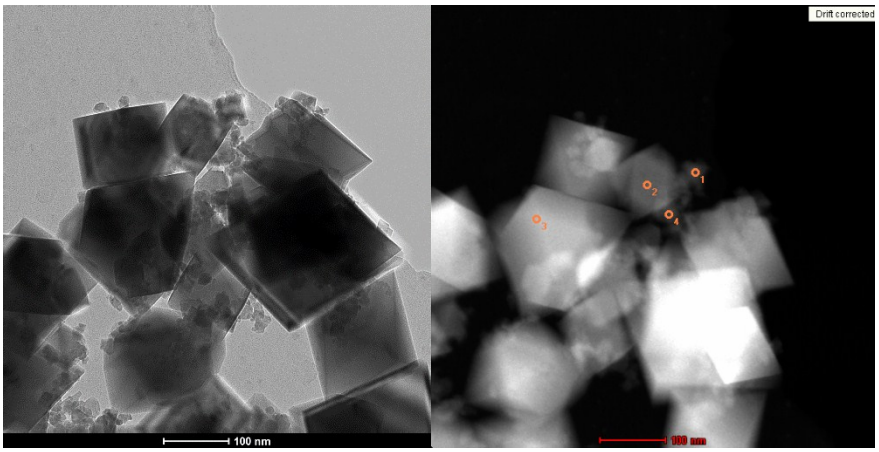

Figure S4. a. TEM image of the $Co_{2+x}Ti_{1-x}O_4$ nano-octahedrons, b. dark field image of corresponding area.

Atomic Proportion	O1		O2		O3		O4	
Ti	35.70	1	31.99	1	27.08	1	31.71	1
Co	64.29	1.80	68.00	2.12	72.91	2.69	68.28	2.15

Table S2. The atomic proportion calculated by EDX by STEM mode.

As we can see by the table above, the component of small irregular particles and regular nano-octahedron particles possessed similar atomic proportions which could prove that the constitutes of irregular particles are similar. The irregular particles are also composed of $Co_{2+x}Ti_{1-x}O_4$ crystalline.

The irregular particles could not be avoid by increasing the reaction time; we can find these small particles from the samples synthesized by 24, 48 and 72 hours. So the relatively broad size distribution of the final product could be caused by the heterogeneous nucleation and secondary nucleation process (Mechanisms of Nucleation and Growth of Nanoparticles in Solution *Chem. Rev.*, 2014, *114* (15), 7610–7630).

The lithium storage capacity of acetylene black was measured under the current of 100 mA/g and shown in the Figure S5. The pure acetylene black without other active materials stably delivered about 260 mAh/g charge/discharge capacity after 10 cycles. The electrode consist of the active material (70 wt. %), conducting agent (acetylene black, 20 wt. %) and binder (polyvinylidene fluoride, PVDF, 10 wt. %); so the extra capacity induced by acetylene black could be calculated to be about 58 mAh/g at the current of 100 mA/g.

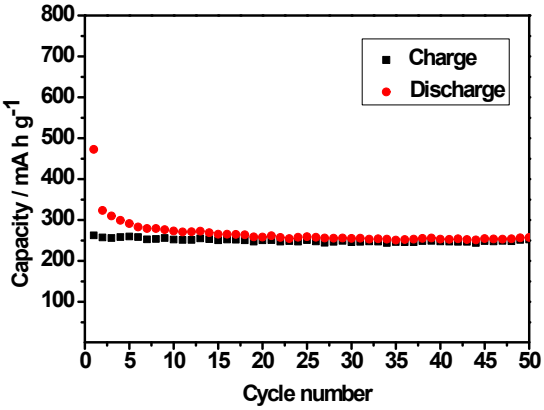

Figure S5. Specific charge/discharge capacity versus cycle number of the acetylene black in the voltage range 0.01-3.0 V at current rate of 100 mA·g^{-1}.

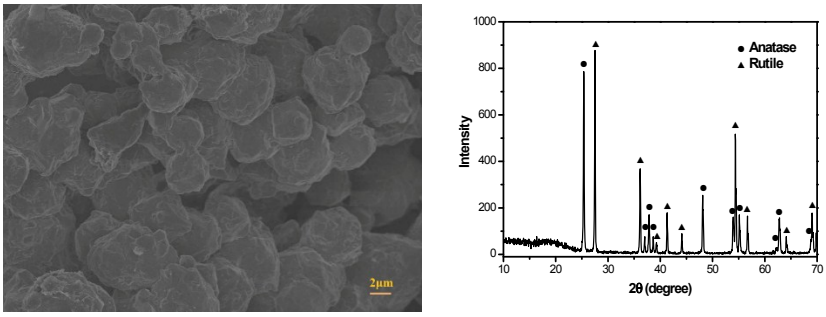

Figure S6. a. SEM image of the raw TiO_2 powder, b. XRD image of the raw TiO_2 powder.